

# Dry powder formulation for pulmonary infections: Ciprofloxacin loaded in chitosan sub-micron particles generated by electrospray

B. Arauzo<sup>a,b</sup>, M.P. Lobera<sup>a,b</sup>, A. Monzon<sup>a</sup>, J. Santamaria<sup>a,b</sup>

<sup>a</sup>*Institute of Nanoscience and Materials of Aragon (INMA) CSIC-Universidad de Zaragoza, Department of Chemical and Environmental Engineering, University of Zaragoza, Campus Río Ebro-Edificio I+D, C/ Mariano Esquillor S/N, 50018 Zaragoza, Spain.*

<sup>b</sup>*Networking Research Center on Bioengineering, Biomaterials and Nanomedicine, CIBER-BBN, 28029 Madrid, Spain.*

**To cite this article:** B. Arauzo, M.P. Lobera, A. Monzon, J. Santamaria. *Dry powder formulation for pulmonary infections: Ciprofloxacin loaded in chitosan sub-micron particles generated by electrospray*, Carbohydrate Polymers 273 (2021) 118543

DOI: 10.1016/j.carbpol.2021.118543

**Disclaimer:** *This is a version of an unedited manuscript that has been accepted for publication. As a service to authors and researchers we are providing this version of the accepted manuscript (AM). Copyediting, typesetting, and review of the resulting proof will be undertaken on this manuscript before final publication of the Version of Record (VoR). During production and pre-press, errors may be discovered which could affect the content, and all legal disclaimers that apply to the journal relate to this version also.*

## **Abstract**

Electrospray was used as a one-step technique to generate inhalable ciprofloxacin-loaded chitosan sub-micron particles with potential use in the treatment of pulmonary infections. The effect of operating parameters was studied and the preparation method optimized. The final sizes of ciprofloxacin-loaded particles were  $386.1 \pm 248.5$  nm and  $501.1 \pm 276.3$  nm for high and low molecular weight chitosan, respectively. The high surface charge of the particles formed, around +45 mV, enhances their mucoadhesive properties. The particles were biocompatible with alveolar cell line (A549), and showed a high antimicrobial activity against two of the most common respiratory pathogens *Staphylococcus aureus* and *Pseudomonas aeruginosa*.

**Keywords:** Chitosan; Electrospray; Ciprofloxacin; Pulmonary administration; Dry powder; Antimicrobial.

## 1. Introduction

Resistance to antibiotics is a serious health problem today, caused by their widespread and sometimes un-appropriate use. This resulted in a decrease of their efficacy, and in the appearance of resistant microorganisms (Alqahtani et al., 2019).

In the last decade, direct pulmonary delivery of antibiotics has raised great interest as an alternative administration route (Douafer, Andrieu, Wafo, & Brunel, 2020). Administration by inhalation in the case of pulmonary infections would allow immediate localization of drugs at the action site with a lower dose of antibiotic, thus reducing side effects and significantly improving patients quality of life (Ling et al., 2019). However, the application of inhaled therapy faces important problems. In particular, delivering the drug at the target site in the respiratory tract is highly challenging. Particle size is considered the main factor in determining the location where the particle will be deposited (Thorley & Tetley, 2013). In this sense, micro and nanosized carriers present important advantages for pulmonary drug delivery such as better pharmacokinetics, controlled release, and reduced uptake by alveolar macrophages, making them suitable candidates for drug delivery in the lungs (De Boer, Gjaltema, Hagedoorn, & Frijlink, 2015; Tu et al., 2015). When alveoli are the target, particles with aerodynamic diameters between 0.02–0.05  $\mu\text{m}$  are expected to have the highest alveolar deposition fraction (~50%) (ICPR, 1994). However, this size (20-50 nm) is extremely difficult to aerosolize as such, since particles in this range tend to aggregate into higher size clusters. A second size range suitable for alveolar deposition is 2–5  $\mu\text{m}$  (~10% of deposition fraction). Interestingly, in both size ranges a large fraction would be deposited outside the alveoli (around 40% for 20-50 nm particles and close to 70% in the 2-5 micron range, respectively) (ICPR, 1994). This opens up another possibility, which is the use of particles in the 200-400 nm (0.2-0.4 micron) range. In this case, a high fraction of the aerosol (ca. 85%) would be expelled again, but most of the rest would deposit in the alveolar region, giving a very significant alveolar deposition yield (ca.~8-10%) with very little load in other pulmonary areas. Thus, a particle size around 300 nm could represent an excellent compromise between alveolar deposition and avoidance of non-selective deposition elsewhere.

A wide variety of polymers is used in pulmonary administration including synthetic such as PLGA (Gaspar et al., 2016) or of natural origin such as chitosan (Gaspar et al., 2015) and alginate (Möbus, Katrin, Siepmann, Jürgen & Bodmeier, 2012). Their structures in

33 any case have to allow biodegradation, in most cases through hydrolytic pathways. In this  
34 work we used chitosan, a natural polymer derived from deacetylation of chitin, it is  
35 formed by D-glucosamide and N-acetylglucosamine units (Grenha, Seijo, & Remuñán-  
36 López, 2005). Chitosan is biodegradable, biocompatible, has low toxicity (LD<sub>50</sub> of 16  
37 g/kg body) and is positively charged thanks to its amino groups (Tawfik & El-Masry,  
38 2021).

39 Electrospray represents one interesting alternative to produce micro – and nanoparticles  
40 by submitting the polymer solution to electric field. When the field reaches a critical  
41 value, repulsive forces between particles overcome the surface tension of solution a spray  
42 is generated and particles can be obtained as a dry powder after solvent removal (Boda,  
43 Li, & Xie, 2018). The particle morphology is influenced by the speed of the drying  
44 process (Pawar, Thakkar, & Misra, 2018). Importantly, electrospraying avoids freeze-  
45 drying and the use of cryoprotectants such mannitol or lactose in the drying process.

46 Chitosan has often been employed to produce fibers (Qasim et al., 2018) and less  
47 frequently particles (Gómez-Mascaraque, Sanchez, & López-Rubio, 2016) by  
48 electrospray. Chitosan is a polymer soluble in acid environments, an important feature,  
49 given the strong role of solvents in electrospraying. Trifluoroacetic acid (TFA) is a strong  
50 acid with a low boiling point (71.8 °C) (Torres-Giner, Ocio, & Lagaron, 2008). It is able  
51 to dissolve chitosan thanks to the formation of salts with its amino groups and lowers  
52 surface tension with respect to acetic acid (Ardila, Ajjí, Heuzey, & Ajjí, 2018).  
53 Furthermore, the addition of dichloromethane (DCM) decreases the dielectric constant  
54 and the conductivity of the mixture, helping the formation of particles rather than fibers  
55 (Torres-Giner et al., 2008).

56 The fundamental hypothesis of this study was that particles of a biodegradable polymer  
57 (chitosan) loaded with antibiotic could be produced by electrospray in a single step  
58 process, yielding inhalable particles of a size suitable to target alveoli. This could have a  
59 strong potential in the treatment of respiratory infections by direct pulmonary delivery of  
60 dry powder formulations. We have chosen ciprofloxacin as the antibiotic used in this  
61 study. It belongs to fluoroquinolones group and it is active against a wide spectrum of  
62 gram (+) and gram (-) bacteria, acting by inhibition of the activity of DNA gyrase and  
63 topoisomerase IV (Pignatello et al., 2018). It is effective against a large number of  
64 microorganisms that have been associated with infections in the respiratory system, such

65 as *Staphylococcus aureus* or *Pseudomonas aeruginosa* (Osman, Kan, Awad, Mortada,  
66 El-Shamy & Alpar, 2013). Nowadays, a single commercial formulation of ciprofloxacin  
67 exists as a dry powder inhaler (DPI) by Bayer AG (Berlin, Germany). Particles of  
68 ciprofloxacin are produced by spray–drying and they combine the novel PulmoSphere™  
69 technology (Novartis) with T-326 inhaler for their administration. This formulation has  
70 demonstrated a decrease in the number of exacerbations in patients with respiratory  
71 bacterial infections (McShane et al., 2018).

72 Our study presents both a different production method and a novel formulation using  
73 ciprofloxacin as an antibiotic for potential use in pulmonary administration against  
74 pulmonary infections by *S. aureus* and *P. aeruginosa*. The use of chitosan would lend the  
75 electrosprayed particles a positive surface charge which is advantageous for their  
76 interaction with the mucus layer in the lungs or with bacteria surfaces that are negatively  
77 charged (Ma, Garrido-Maestu, & Jeong, 2017). In addition, the formulation used in this  
78 work avoids the use of excipients. Last but not least, the electrospray method allows to  
79 obtain particles with a controlled size (Moreno et al., 2018). Thus, this one-step  
80 production technique yielded drug-loaded particles with a narrow distribution  
81 approaching a size that represents, as shown above, an excellent choice for alveolar  
82 deposition.

## 83 **2. Materials and Methods**

### 84 **2.1 Materials**

85 Reagents, high molecular weight chitosan (HMW\_CS) (deacetylation degree:  $\geq 75\%$ ;  
86 viscosity: 800–2000 cP 1wt.% in 1% acetic acid), low molecular weight chitosan  
87 (LMW\_CS) (deacetylation degree: 75–85%; viscosity 20–300 cP 1wt.% in 1% acetic  
88 acid), phosphate buffered saline tablets (PBS) (pH 7.4) and trifluoroacetic acid (TFA)  
89 were purchased from Sigma–Aldrich (USA); dichloromethane (DCM; Fisher Chemicals,  
90 UK) and ciprofloxacin (1-cyclopropyl-6-fluoro-4-oxo-7-piperazin-1-ylquinoline-3-  
91 carboxylic acid, CPX; Fluka analytical, Spain).

92 Bacteria strains, *Staphylococcus aureus* (ATCC 25923; Ielab, Spain) and *Pseudomonas*  
93 *aeruginosa* (ATCC 10145; Ielab, Spain). Cell line A549 (ATCC–CCL–185) were kindly  
94 provided by Dr. P. Martin-Duque and used between passages 25–32.

### 95 **2.2 Electrospray production of chitosan-based sub-micron particles**

96 Electrospinning was performed in Yflow 2.2D-500 electrospinner (Coaxial  
97 Electrospinning Machines/R&D Microencapsulation, Spain). Briefly, electrospinning of  
98 different chitosan solutions in a TFA/DCM mixture was conducted at diverse flow rates  
99 controlled by a syringe pump. The needle (0.6 mm, inner diameter) was positioned  
100 vertically towards the grounded collector plate and connected to the positive electrode  
101 and the negative electrode was connected to a stationary collector plate located at a certain  
102 distance from the needle tip. All experiments were conducted at RT, (HR)% of 25-50%  
103 and under atmospheric pressure. Preliminary experiments allowed the optimization of  
104 some operational parameters such as tip-to-collector distance (H) and applied voltage (V).  
105 The reference set of conditions for electrospinning CS solutions are H= 10 cm and V: 9-  
106 27 kV.

107 The effect of chitosan MW, flow rate and polymer concentration were studied to evaluate  
108 their influence in particle size distribution and to select the best conditions to produce  
109 chitosan sub-micron particles (CS SMPs) reducing the appearance of large beads and  
110 especially of fibers. This study was carried out with empty (ciprofloxacin-free) chitosan  
111 particles. To do that, electrospinning of diverse solution of HMW and LMW chitosan  
112 (from 20 mg/mL to 50 mg/mL) in a mixture of TFA/DCM (70% v/v of TFA) was  
113 conducted using flow rates between 0.2 mL/h and 1 mL/h. *Table S1 (Supplementary*  
114 *Information (SI))* shown different electrospinning parameters evaluated.

115 Once the conditions were optimized to obtain spherical CS SMPs with a suitable size  
116 range, CPX was added to the electrospinning solution. CPX concentrations from 1 mg/mL  
117 to 10 mg/mL were tested. All the other parameters were kept constant.

### 118 **2.3 Characterization of chitosan sub-micron particles**

119 FTIR analysis of chitosan, raw ciprofloxacin and chitosan SMPs were made using Vertex-  
120 70 FTIR spectrophotometer (Brucker, USA). Each spectrum was analysed with a  
121 resolution 4 cm<sup>-1</sup> and 40-scan.

122 Scanning electron microscopy (SEM) was conducted on a FEI Inspect Field Emission  
123 instrument at accelerating voltages between 5-10 kV to obtain the morphology and size  
124 distribution of all prepared materials. Samples were sputter-coated with Palladium (Pd).

125 Zetasizer Nano ZS<sup>®</sup> (Malvern Instruments, UK) was used to measure the particle size  
126 (photon correlation spectroscopy) and Zeta potential (laser doppler anemometry). For the  
127 particle size analysis, each sample was diluted in ultrapure water and sonicated before the  
128 measurement. Zeta potential value was measured in a mixture of water and 1 mM KCl  
129 and placed in the electrophoretic cell.

#### 130 **2.4 Encapsulation efficiency (%EE) and drug loading (%DR)**

131 Drug content was determined by extracting all the ciprofloxacin from the SMPs in acidic  
132 medium (0.1M HCl). 1 mg of SMPs loaded with CPX was added to 2 mL of 0.1M HCl.  
133 The suspension was stirred at 500 rpm for 48 h at RT. Finally, solution was centrifuged  
134 10 min at 13000 rpm and the supernatant was recovered.

135 The absorbance of CPX in the supernatant was measured at 277 nm on a  
136 spectrophotometer (PerkinElmer Lambda-35) and the concentration of CPX was  
137 calculated using its standard curve. %EE and %DR of SMPs were calculated as follows:

$$138 \quad \%EE = (\text{Measured mg ciprofloxacin} / \text{Theoretical mg ciprofloxacin}) \cdot 100$$

$$139 \quad \%DR = (\text{Measured mg ciprofloxacin} / \text{mg SMPs}) \cdot 100$$

#### 140 **2.5 In vitro drug release studies**

141 *In vitro* drug release study was conducted in PBS. Suspensions of 1 mg/mL of CPX-  
142 loaded SMPs were incubated at 37 °C under horizontal shaking at 250 rpm. At fixed times  
143 (0, 15, 30, 45 minutes and 1, 2, 4, 6, 8, 24, 48, 72 h), these suspensions were centrifuged  
144 (13000 rpm for 10 min, at RT). The CPX content was obtained by measuring the  
145 supernatants.

#### 146 **2.6 Bacteria cultures and assays for antimicrobial activity**

147 Antimicrobial activity of chitosan particles and raw ciprofloxacin was evaluated in gram  
148 (+) bacteria model, *S. aureus* and gram (-) bacteria model, *P. aeruginosa* by determining  
149 of minimum inhibitory concentration (MIC) and minimum bactericidal concentration  
150 (MBC) values.

151 Both strains were grown for 16 h in TSB in a shaker (Innova® 40, New Brunswick  
152 Scientific) with 150 rpm and 37 °C. Finally, 10<sup>8</sup>-10<sup>9</sup> colony-forming units/mL (CFU/mL)  
153 were obtained.

154 The grown bacteria were diluted in TSB to a final concentration of ~10<sup>5</sup> CFU/mL.  
155 Different concentrations of CPX-loaded HMW\_CS SMPs and raw CPX (0.125, 0.250,  
156 0.375, 0.500, 0.750 and 1 µg/mL) were inoculated with *S. aureus* and CPX-loaded  
157 LMW\_CS SMPs and raw CPX (0.0625, 0.125, 0.250, 0.500, 1, 2, 4 and 8 µg/mL) with  
158 *P. aeruginosa*.

159 Control A group was bacteria not exposed to any study sample and control B group was  
160 bacteria exposed to the volume of 0.1M HCl solution necessary to dissolve raw CPX,  
161 both control groups were included to confirm correct growth of the bacteria.

162 The optical densities of pathogenic bacteria in contact with SMPs and raw drug were  
163 measured at 600 nm (Implen<sup>TM</sup> OD600; ThermoFisher Scientific) to examine bacteria  
164 growth. To this end, *S. aureus* and *P. aeruginosa* (~10<sup>5</sup> CFU/mL) were inoculated in each  
165 sample. The mixed suspensions were kept in a shaker at 37 °C at 150 rpm and OD<sub>600</sub> was  
166 measured at selected times up to 24 h.

167 Agar dilution method allowed to quantify the number of CFU/mL and it was also used to  
168 evaluate the antimicrobial activity of CPX-loaded in CS SMPs. The bacteria were diluted  
169 to ~10<sup>5</sup> CFU/mL and then inoculated with different samples. Bacteria were kept in a  
170 shaker at 37 °C at 150 rpm during 24 h. After that, bacteria suspensions were diluted in  
171 PBS and seeded in Petri plates with TSA at 37 °C for 24 h. The MBC was determined by  
172 testing the concentration that showed no visible bacteria growth (the lowest concentration  
173 that kills > 99.95 of the bacteria)

## 174 **2.8 In vitro cytotoxicity assay on A549 cells**

175 A549 cell viability after exposure to the prepared CS SMPs were used to assess their  
176 toxicity, using the Alamar Blue assay. A549 is a human alveolar epithelium cell line,  
177 often employed in cytotoxicity studies. The cell culture medium (CCM) was DMEM with  
178 FBS (10% v/v) and antimitotic-antibiotic, penicillin (60 µg/mL), streptomycin (100  
179 µg/mL) and amphotericin B (0.25 µg/mL).



180 A549 cells were seeded into a 96-well plate at a density of  $1 \times 10^4$  cells/well in 100  $\mu$ L  
181 CCM for 24 h and 48 h in a CO<sub>2</sub> incubator. Cells were allowed to attach for 24 h. The  
182 samples were sterilized by UV irradiation at least 30 min before contacting with cells.  
183 Raw CPX, CS SMPs and CPX-loaded CS SMPs were dispersed in CCM at different  
184 selected concentrations (0.1  $\mu$ g/mL – 100  $\mu$ g/mL). The CCM was replaced with the new  
185 culture medium containing the particles. Four wells with cells not exposed to any sample  
186 were used as controls in each experiment.

187 After that, the medium was removed and the cells were washed twice with DPBS. Then,  
188 the Alamar Blue reagent was added following the manufacturer's indications (10% v/v;  
189 incubation at least 1 h at 37 °C and 5% CO<sub>2</sub>). A microplate reader (Multimode Synergy  
190 HT Microplate Reader; Biotek, USA), at  $\lambda_{530}$  nm excitation and  $\lambda_{590}$  nm emission, was  
191 used to record the fluorescence displayed. The viability was calculated by linear  
192 interpolation of the mean fluorescence values (MFV) from the cells treated with SMPs  
193 and raw ciprofloxacin versus the untreated one:

$$194 \quad \% \text{ Cell viability} = (\text{MFV of treated cells} / \text{MFV of control cells}) \cdot 100$$

195 To determine the toxicity threshold, the ISO 10993-5 norm was used (Biological  
196 evaluation of medical devices – Part 5: Tests for in vitro cytotoxicity). This norm  
197 considers a material as non-cytotoxic when cellular viability is >70%.

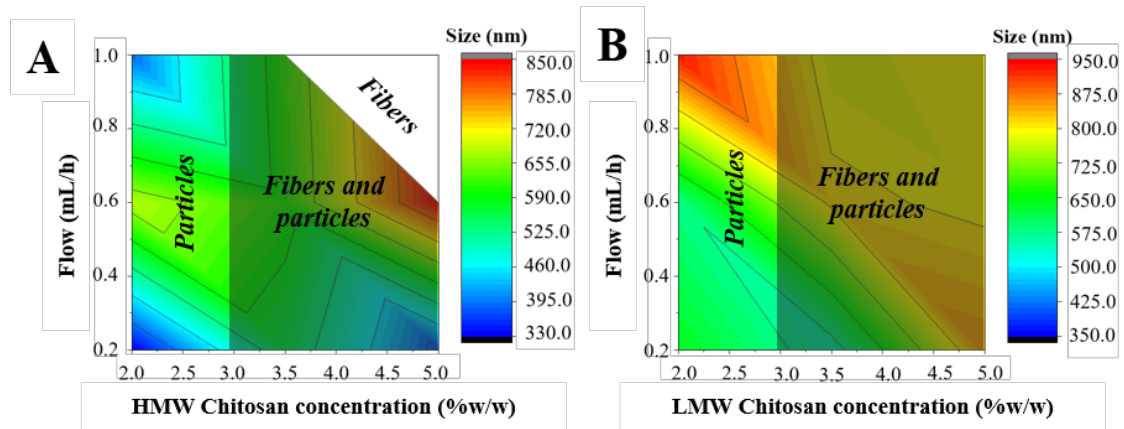
### 198 **3. Results and discussion**

#### 199 **3.1 Electrospayed unloaded chitosan sub-micron particles**

200 The chitosan concentration was varied from 2% w/w to 5% w/w. The feed flow rate could  
201 be increased up from 0.2 to 1 mL/h thanks to the higher stability of the Taylor cone with  
202 TFA/DCM. A set of 18 different experimental electrospay parameters was tested (*Table*  
203 *S2*). The morphology of electrospayed materials and particle size obtained are shown in  
204 *Tables S3, S4* and *Figures S1, S2* in *SI*.

205 For both molecular weight of chitosan tested (HMW\_CS and LMW\_CS), it is possible to  
206 observe the effect of the chitosan concentration and flow rate on the morphology of the  
207 material obtained (*Figure 1*). The main controlling parameter is chitosan concentration  
208 and in fact for CS up to around 3 % w/w the fiber formation can be avoided for the whole  
209 interval of flow rates investigated (0.2 to 1 mL/h) and irrespective of the MW of chitosan

210 used. However, it can be seen that, for HMW\_CS, in the region of high CS concentrations  
211 and flow rates, nanofibers are obtained, almost exclusively.



212

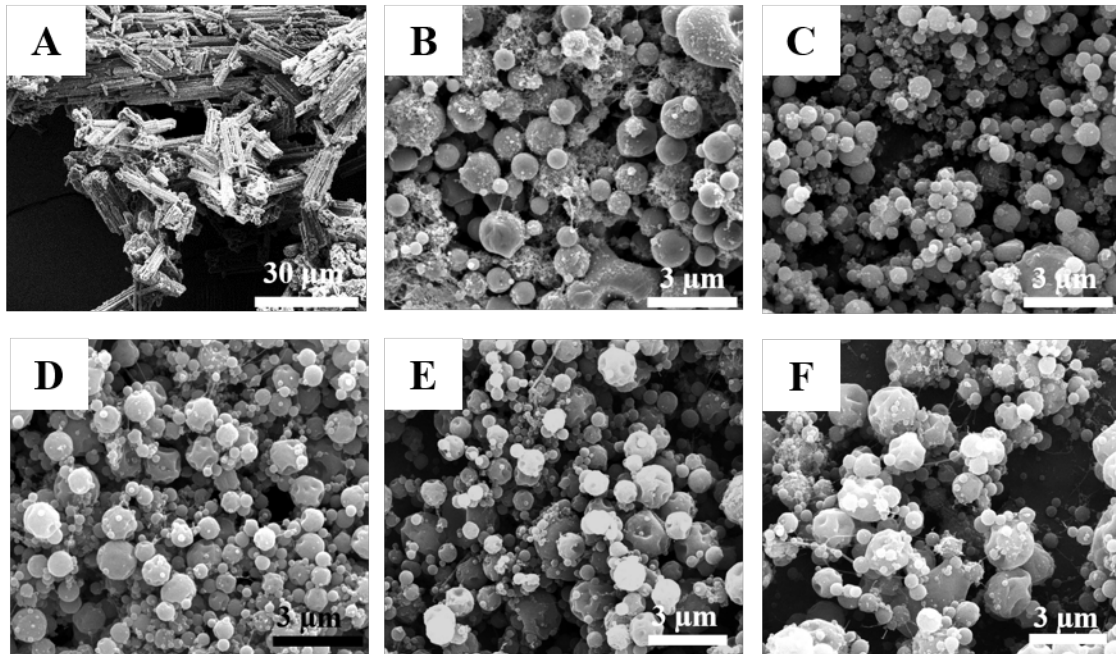
213 Fig. 1. Flow (mL/h) and polymer concentration (% w/w) influence on particle size diameter for  
214 different molecular weight chitosan. (a) HMW chitosan; (b) LMW chitosan.

215 In both systems, the region of low concentrations of chitosan (~2% w/w) and low flow  
216 rates (0.2 mL/h) produced small particles with spherical morphology and narrow size  
217 distribution (formulations H02/20 and L02/20 in *SI*). On the other hand, higher chitosan  
218 concentrations above 3 % w/w led to a mixture of particles and interconnected fibers as  
219 seen in *Figures S1* and *S2*.

220 In summary, a concentration of chitosan 2% w/w, flow rate of 0.2 mL/h were selected as  
221 optimal to produce the particles in this work. This led to fine spherical chitosan particles  
222 with a size well that could be inhaled for pulmonary administration. To test the aerosol  
223 behaviour of these particles and their aerodynamic diameter, a sample of 10 mg was  
224 loaded into a pressure-pulse aerosol generator (Clemente, Lobera, Balas, & Santamaria,  
225 2018) and dispersed while measuring the particle size distribution. The results are shown  
226 in *Figure S3*, where it can be seen that the aerosolized particles present a bimodal size  
227 distribution with peaks at  $73 \pm 9$  nm, and at  $195 \pm 80$  nm respectively. This is a  
228 consequence of the aerosolization process used, that projects the particles through a  
229 narrow opening with a high shear stress and may vary with operating conditions, but in  
230 any case, these sizes would also be in a similar range regarding alveolar deposition.

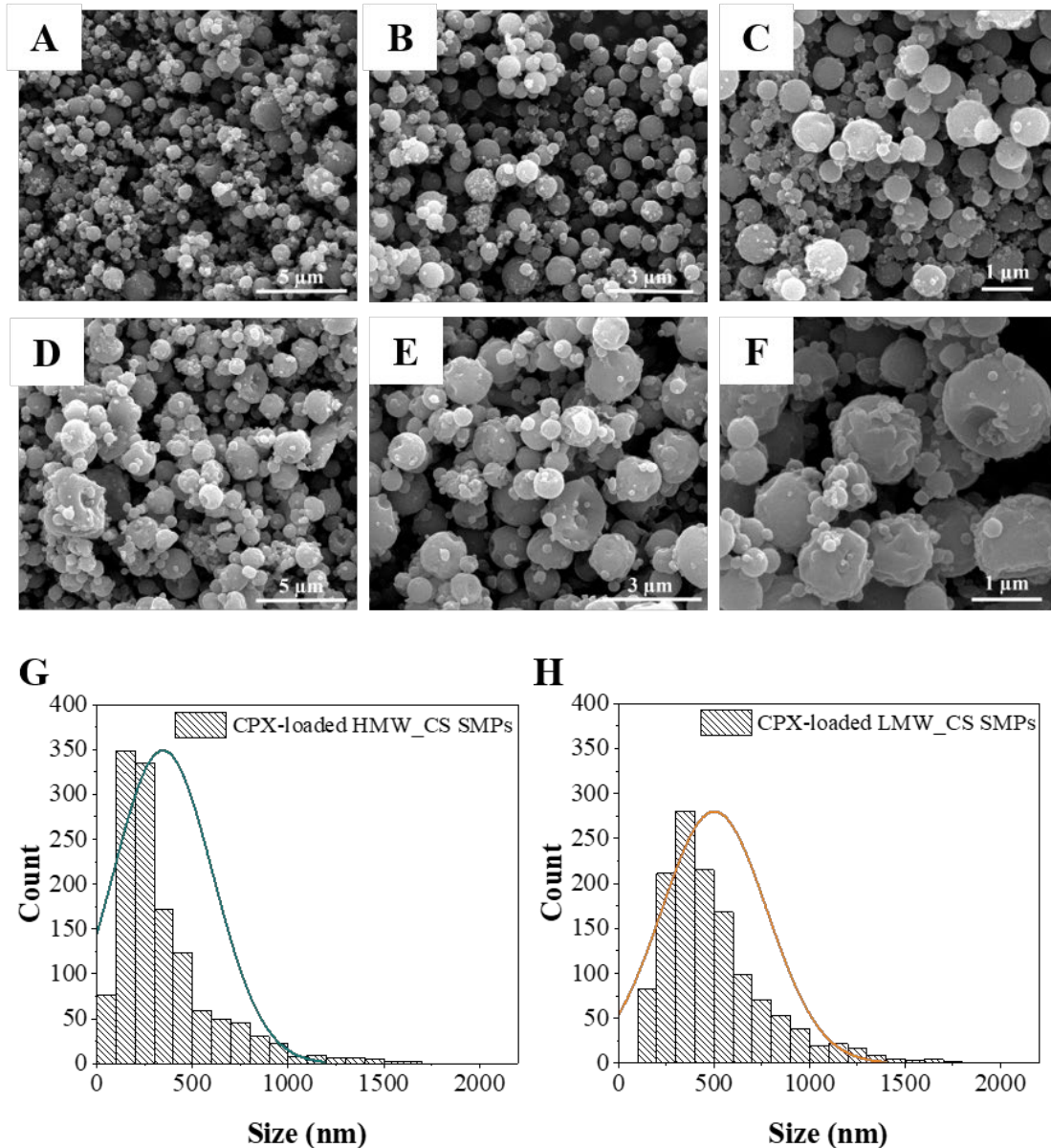
### 231 3.1.2 Ciprofloxacin-loaded chitosan sub-micron particles

232 Using the reference set of electrospray parameter, CPX was added to the electrospray  
233 solution (concentrations from 1 mg/mL to 10 mg/mL). Spherical, well-formed particles  
234 were obtained with increasing concentrations of CPX. Interestingly, the morphology with  
235 different CPX concentrations was very similar to that obtained for empty chitosan  
236 particles. For this reason, the conditions for the production of SMPs could be extended to  
237 a concentration of 5 mg/mL of CPX, enabling a higher drug loading (*Figure 2*).



238  
239 Fig. 2. SEM images (a) Pristine ciprofloxacin; (b-f) Electrospun chitosan particles prepared  
240 with different concentration of ciprofloxacin; (b) 10 mg/mL; (c) 5 mg/mL; (d) 4 mg/mL; (e) 2  
241 mg/mL; (f) 1 mg/mL.

242 Using the reference conditions, the electrospraying experiments were repeated with  
243 HMW and LMW chitosan. The results are shown in *Figure 3*. As can be seen, LMW\_CS  
244 always gives rise to larger particles for both empty and loaded SMPs compared to  
245 HMW\_CS.



246

247 Fig. 3. SEM images of chitosan particles. (a - c) CPX-loaded HMW\_CS SMPs; (d - e) CPX-  
 248 loaded LMW\_CS SMPs. (g and h) Size distribution particles

### 249 3.2 Characteristics and morphology properties of CPX-loaded particles

250 FTIR chitosan powder spectra showed a characteristic band in region  $3400-3200\text{ cm}^{-1}$   
 251 attributed to  $-\text{NH}_2$  and  $-\text{OH}$  groups,  $2920\text{ cm}^{-1}$  (C-H stretching) and amide I ( $1640\text{ cm}^{-1}$ )  
 252  $^1$ ). Raw ciprofloxacin showed a main peak at  $1286$  due to the C-F bond (Kyzioł, Mazgała,  
 253 Michna, Regiel-Futyra, & Sebastian, 2017). CS SMPs and CPX-loaded CS SMPs  
 254 displayed a shifted band from  $1640\text{ cm}^{-1}$  to  $1660\text{ cm}^{-1}$  corresponding to the presence of  
 255 chitosan in both SMPs. However, when CPX was loaded the CS SMPs spectrum revealed

256 a characteristic band at 1286 cm<sup>-1</sup> (C–F bond), confirming the presence of ciprofloxacin  
 257 in the loaded particles. Also, chitosan particles presented bands corresponding on one  
 258 side to N-H stretching (including NH<sub>4</sub><sup>+</sup>) at 1660–1520 cm<sup>-1</sup> and the other to C–O  
 259 stretching of C<sub>2</sub>F<sub>3</sub>O<sub>2</sub><sup>-</sup> (bands at 1190–890 cm<sup>-1</sup>) (Torres-Giner et al., 2008). The presence  
 260 of these active groups (NH<sub>4</sub><sup>+</sup> and C<sub>2</sub>F<sub>3</sub>O<sub>2</sub><sup>-</sup>) in CS SMPs could give rise to some  
 261 antimicrobial activity caused by the particle material itself (*Figure S4* in *SI*).

262 *Table 1* shows the main results from the characterization of the SMPs. Irrespective of the  
 263 loading, the key factor regarding particle size is the MW of CS used, with considerably  
 264 larger particles with LMW\_CS. Torres-Giner et al. (2008) showed that an increase in the  
 265 MW of chitosan in a TFA/DCM solution produced an increase in the viscosity and  
 266 decreased the surface tension. As a consequence, with HMW\_CS is easier to obtain fibers  
 267 and smaller particles, while the formation of larger particles is more likely when  
 268 LMW\_CS is used. Indeed, in the case of LMW the SMPs obtained were almost twice the  
 269 size of the HMW\_CS SMPs. Particles with this size (< 1µm) are normally deposited in  
 270 the lower respiratory system such as bronchioles and alveoli (Klinger-Strobel et al., 2015;  
 271 Yhee, Im, & Nho, 2016).

272 As shown in *Table 1*, both types of SMPs are positively charged due to the amino groups  
 273 of chitosan. This is an important advantage for biomedical applications since it favours  
 274 interactions between chitosan particles and surfaces of the lung mucus layer or bacteria,  
 275 both negatively charged (George & Abraham, 2006). The strong positive surface charge  
 276 (in excess of +40 mV and in some cases higher than +50 mV) of these SMPs also helps  
 277 to prevent agglomeration, as shown by the DLS values, giving sizes in solution are less  
 278 than twice those of individual particles, i.e. the solution is largely made of dispersed  
 279 individual particles.

280 **Table 1**

281 Properties of chitosan sub-micron particles used in this study.

Sample	SEM	Z potential	DLS	EE	DL
	<i>Mean ± SD</i> (nm)	(mV)	<i>Mean ± SD</i> (nm)	(%)	(%)
CPX	-	12.1 ± 4.5	-	-	-
HMW_CS SMPs	333.9 ± 217.9	51.0 ± 11.2	438.0 ± 81.2	-	-

CPX-loaded HMW_CS SMPs	386.1 ± 248.5	42.1 ± 5.2	625.1 ± 68.6	75.6 ± 10.2	15.8 ± 2.1
LMW_CS_SMPs	636.3 ± 312.4	42.6 ± 6.2	596.2 ± 100.7	-	-
CPX-loaded LMW_CS SMPs	501.1 ± 276.3	52.0 ± 10.5	533.3 ± 39.1	70.5 ± 16.5	14.1 ± 3.3

### 282 3.4 In vitro release studies: mechanism and kinetics

283 Many mathematical models have been used to describe and/or design drug delivery  
284 systems and to predict the overall release behaviour as a function of time. A realistic  
285 model therefore becomes a key tool to tune release patterns in a way that matches the  
286 therapeutic regimen of patients.

287 In this work, the kinetics of ciprofloxacin release from chitosan SMPs were initially fitted  
288 to Linder-Lippold (Linder & Lippold, 1995), Ritger-Peppas (Korsmeyer, Meerwall, &  
289 Peppas, 1986), and Peppas-Sahlin (Peppas & Sahlin, 1989) empirical models (*Table S5 in*  
290 *SI*). The fitting of the experimental data of ciprofloxacin concentration ( $m_t$ ) versus time  
291 with the above models was not good ( $R^2 < 0.900$ ), in spite of the number of adjustable  
292 parameters used (2 or 3 depending on model).

293 In order to have a more realistic description of kinetics release, we have assumed that the  
294 rate of ciprofloxacin released from the chitosan particles, ( $dm^s/dt$ ), is a first order process,  
295 and therefore the content of ciprofloxacin in the chitosan particles decays exponentially  
296 along time:

$$297 \quad -dm^s/dt = k_R \cdot m^s_t \rightarrow m^s_t = m^s_0 \cdot \exp(-k_R \cdot t)$$

298 In the above equation  $m^s_0$  represents the initial ciprofloxacin in the chitosan particles and  
299  $k_R$  is the kinetic constant of drug release. This parameter depends of the specific  
300 interaction developed between the substrate (chitosan) and the drug released  
301 (ciprofloxacin), and also on the operational conditions of the kinetic experiments. In fact,  
302 this is the only one parameter that is calculated by non-linear regression of the model to  
303 the experimental data. The amount of ciprofloxacin released to the solvent can be now  
304 calculated directly from the mass balance as follows:

$$305 \quad m_t = m^s_0 - m^s_t \rightarrow m_t = m^s_0 \cdot (1 - \exp(-k_R \cdot t)); \quad m^s_0 = m_\infty$$

306 From this equation it is deduced that the maximum concentration of ciprofloxacin  
307 attainable,  $m_\infty$ , corresponds to the initial amount loaded on the chitosan particles,  $m^s_0$ .

308 On *Table 2* the values of  $k_R$ ,  $m_\infty$  and  $R^2$  are presented for the two samples of chitosan  
309 studied. The higher values of  $R^2$  obtained with the one-parameter exponential model, in  
310 comparison with the above models suggests the validity of the assumptions made here  
311 (curve fittings for the different models are graphically displayed in *Figure S5*).

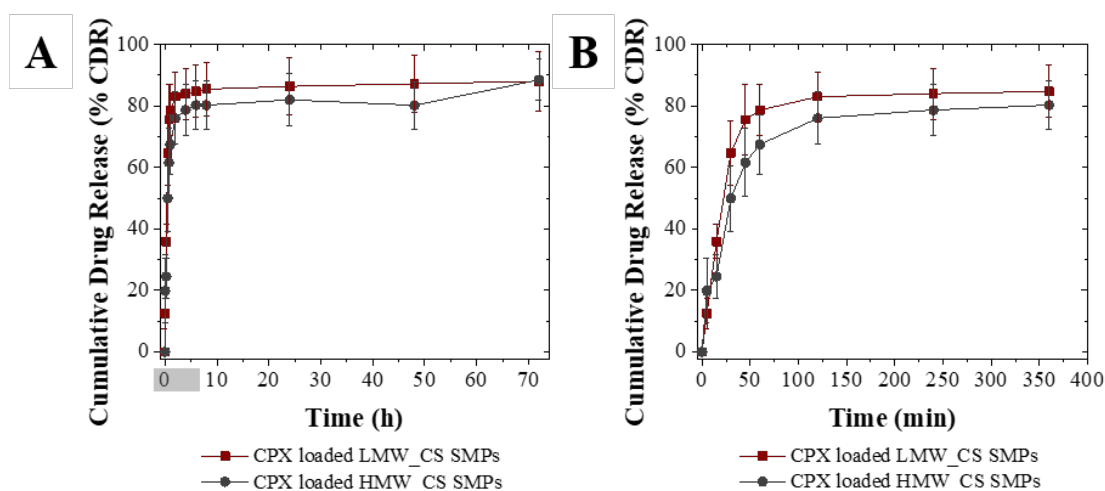
312 According to this model, the intrinsic rate of chitosan release from the LMW\_CS sample  
313 is around 37% higher than of the HMW\_CS sample, indicating a lower interaction  
314 between the chitosan and the ciprofloxacin on the LMW case. As expected, the estimated  
315 values of  $m_\infty$  are in agreement with the experimental values of  $m^s_0$  used in each case.

316 **Table 2**

317 Kinetic constant of ciprofloxacin release for the HMW and LMW chitosan samples.

<i>Sample</i>	$k_R \pm SE$ (min <sup>-1</sup> )	$m_\infty \pm SE$ (% mg)	$R^2$	<i>ner. points</i>
<i>CPX-loaded HMW_CS SMPs</i>	0.0303 ± 0.0026	81.237 ± 1.607	0.970	104
<i>CPX-loaded LMW_CS SMPs</i>	0.0416 ± 0.0022	85.938 ± 0.957	0.995	65

318 Ciprofloxacin release could be enhanced by dissolution of chitosan chains. According to  
319 Jayakumar et al., (2010) chitosan structures prepared by electrospray showed a fast and  
320 complete dissolution in contact with neutral or weak basic aqueous solutions. This could  
321 explain the rapid release observed for CPX in this work. *Figure 4* shows the cumulative  
322 drug release (%CDR) for the two kind of chitosan SMPs at 37 °C as a function of time.  
323 A quick release of ciprofloxacin from chitosan SMPs is an advantage when the objective  
324 is the treatment of acute bacterial infections, since the antibiotic being released shortly  
325 after inhalation.



326

327 Fig. 4. Cumulative drug release (%CDR) in PBS with respect to total encapsulated drug for two  
 328 different molecular weight chitosan SMPs (n = 3); (a) %CDR until 72 hours; (b) %CDR until 6  
 329 hours.

### 330 3.5 Determination of minimum inhibitory concentrations (MIC) and minimum 331 bactericidal concentrations (MBC)

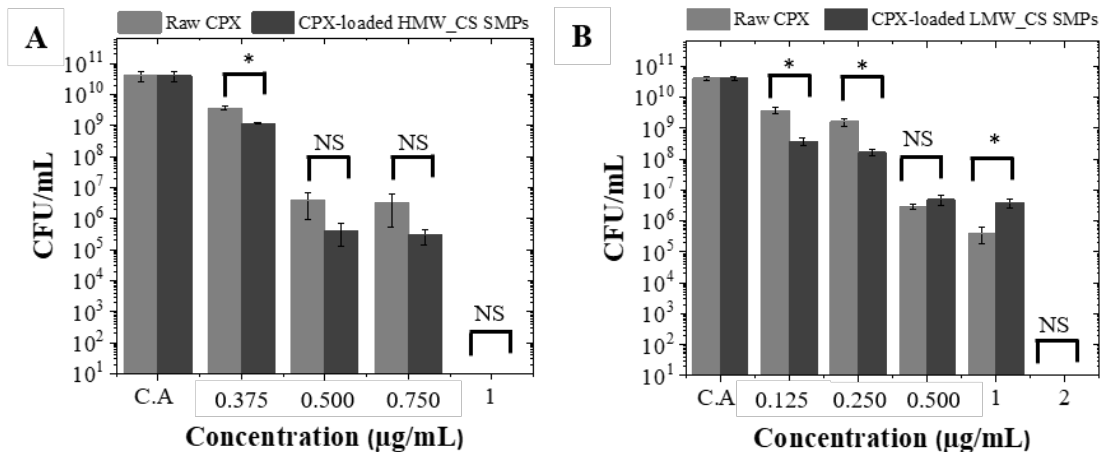
332 The antibacterial activity of chitosan SMPs was tested against two important pathogens  
 333 (*S. aureus* and *P. aeruginosa*) in lung infections. In the case of gram (+) strains, previous  
 334 studies showed that the positive charge of chitosan interacts with the negative charge of  
 335 the bacterial wall, producing a change in the permeability of the wall and facilitates the  
 336 exit of intracellular components. In contrast, for gram (-) strains chitosan is able to cross  
 337 the cell membrane and act from the inside, also promoting the exit of cellular material  
 338 (Verlee, Mincke, & Stevens, 2017).

339 Growth curves (Figure S6) showed that *S. aureus* at 0.250 and 0.375 (MIC)  $\mu\text{g/mL}$   
 340 displayed a lag phase up to 16 h, indicating that the growth bacteria was inhibited and the  
 341 log phase was delayed. In the case of *P. aeruginosa*, at 0.250 (MIC)  $\mu\text{g/mL}$  the log phase  
 342 was delayed up to 12 h. However, from 0.500  $\mu\text{g/mL}$  it was not possible to distinguish  
 343 between the lag and log phases. This result showed that *S. aureus* and *P. aeruginosa* were  
 344 more susceptible to the exposure to SMPs when compared to raw ciprofloxacin. Those  
 345 concentrations where a strong decrease in bacterial growth was observed were studied  
 346 with the agar dilution method. 1  $\mu\text{g/mL}$  (MBC) was the concentration found to inhibit the  
 347 growth bacteria (Figure 5).



348 It can be concluded that ciprofloxacin encapsulated in chitosan SMPs not only retained  
 349 its antimicrobial activity but also the encapsulated formulations were effective in short  
 350 periods of time.

351



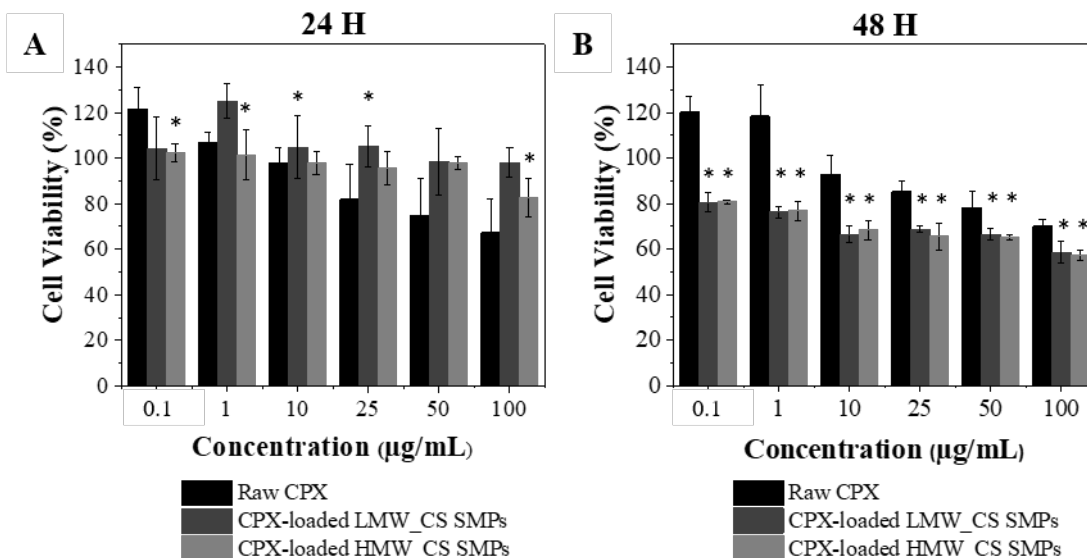
352

353 Fig. 5. Antibacterial activity (CFU/mL) of CPX (raw and encapsulated). (a) *S. aureus*; (b) *P.*  
 354 *aeruginosa* (mean ± SD, n = 3; p\* < 0.05; NS, no significant difference).

### 355 3.6 Cytotoxicity assay

356 Finally, a cytotoxicity assay was carried out to study the biocompatibility of CPX-loaded  
 357 CS SMPs. Raw ciprofloxacin was also tested. Concentration tested were 50 times the  
 358 MBC (2 μg/mL) found for these SMPs.

359 *Figure 6* shows the cell viability percentages obtained after 24 h and 48 h. It can be seen  
 360 that, after 24 h of exposure to the different samples, only raw ciprofloxacin showed  
 361 cytotoxicity at the highest concentration of 100 μg/mL. However, after 48 h, CPX-loaded  
 362 HMW\_CS SMPs and CPX-loaded LMW\_CS SMPs were found to be cytotoxic from 10  
 363 μg/mL, while at the same time of exposure, raw ciprofloxacin showed cytotoxicity at 100  
 364 μg/mL. However, it must be considered that the limit of toxicity (10 μg/mL), is 10 times  
 365 of the MBC for *S. aureus* and 5 times of the MBC for *P. aeruginosa*. i.e., for  
 366 concentrations lower than 10 μg/mL, *S. aureus* and *P. aeruginosa* will still die while the  
 367 environment would be non-toxic to respiratory cells.



368

369 Fig. 6. Cell viability studies of raw CPX and CPX encapsulated in SMPs. Exposure time: (a) 24  
 370 h; (b) 48 h. Significant differences ( $p < 0.05$ ) between different samples tested in relation to raw  
 371 CPX (mean  $\pm$  SD,  $n = 3$ ).

#### 372 4. Conclusions

373 This study presents a new method to produce dry chitosan SMPs loaded with  
 374 ciprofloxacin. The particles were produced by electrospray as a dry powder in just one-  
 375 step and were excipient-free. This method yielded a particle size that would be in principle  
 376 suitable to reach alveoli, with reduced deposition elsewhere in the lung. The CPX-loaded  
 377 chitosan SMPs showed potent antimicrobial activity against *S. aureus* and *P. aeruginosa*.  
 378 CPX release was fast (50% release was achieved in 30 min) and can be characterized as  
 379 a first order release process. Cytotoxicity assays in A549 human lung epithelial cells  
 380 showed that ciprofloxacin-containing chitosan particles are safe to be used at the MBC  
 381 doses. In summary, the results indicate that electrospraying of CS with CPX solutions  
 382 using TFA/DCM mixtures as solvents yields SMPs of a size suitable for pulmonary  
 383 delivery by inhalation, with a high drug content (around 15%) and encapsulation  
 384 efficiency above 75%.

#### 385 Acknowledgments

386 Financial support from Nanbiosis platform and Center for Network Research in  
 387 Bioengineering, Biomaterials and Nanomedicine (CIBER-BBN). B. Arauzo thanks DGA  
 388 predoctoral fellowship for personal researcher (2017-2021). Authors thank the

389 "Advanced Microscopy Laboratory" of the "Institute of Nanoscience and Materials of  
390 Aragon - University of Zaragoza", LMA-INMA, for access to their instruments. Finally,  
391 authors thank Dr. Pilar Martín-Duque for kindly providing A549 cells and also Dr.  
392 Manuel Arruebo, Dr. Gracia Mendoza and Dr. Cristina Yus for offering their expertise.

393

## 394 **References**

395 Alqahtani, F. Y., Aleanizy, F. S., Tahir, E. E., Alquadeib, B. T., Alsarra, I. A., Alanazi, J. S., &  
396 Abdelhady, H. G. (2019). Preparation, characterization, and antibacterial activity of  
397 diclofenac-loaded chitosan nanoparticles. *Saudi Pharmaceutical Journal*, 27(1), 82–87.  
398 <https://doi.org/10.1016/j.jsps.2018.08.001>

399 Ardila, N., Ajji, Z., Heuzey, M.C., Ajji, A. (2018). Chitosan electrospraying: Mapping of process  
400 stability and micro and nanoparticle formation. *Journal of Aerosol Science*, 126, 85–98.

401 Boda, S. K., Li, X., & Xie, J. (2018). Electrospraying an enabling technology for pharmaceutical  
402 and biomedical applications: A review. *Journal of Aerosol Science*, 125(April), 164–181.  
403 <https://doi.org/10.1016/j.jaerosci.2018.04.002>

404 Clemente, A., Lobera, M. P., Balas, F., & Santamaria, J. (2018). A versatile generator of  
405 nanoparticle aerosols. A novel tool in environmental and occupational exposure assessment.  
406 *Science of the Total Environment*, 625, 978–986.  
407 <https://doi.org/10.1016/j.scitotenv.2017.12.125>

408 De Boer, A. H., Gjaltema, D., Hagedoorn, P., & Frijlink, H. W. (2015). Can “extrafine” dry  
409 powder aerosols improve lung deposition? *European Journal of Pharmaceutics and*  
410 *Biopharmaceutics*, 96, 143–151. <https://doi.org/10.1016/j.ejpb.2015.07.016>

411 Douafer, H., Andrieu, V., Wafo, E., & Brunel, J. M. (2020). Characterization of a new aerosol  
412 antibiotic/adjuvant combination for the treatment of *P. aeruginosa* lung infections.  
413 *International Journal of Pharmaceutics*, 586(April), 119548.  
414 <https://doi.org/10.1016/j.ijpharm.2020.119548>

415 Gaspar, M. C., Grégoire, N., Sousa, J.J.S., Pais, A. A. C. C., Lamarche, I., Gobin, P., Olivier, J.  
416 C., Marchand, S., Couet, W. (2016). Pulmonary pharmacokinetics of levofloxacin in rats  
417 after aerosolization of immediate-release chitosan or sustained-release PLGA microspheres.  
418 *European Journal of Pharmaceutical Sciences*, 93, 184–191.

- 419 <https://doi.org/10.1016/j.ejps.2016.08.024>
- 420 Gaspar, M. C., Sousa, J. J. S., Pais A. A. C. C., Cardoso, O., Murtinho, D., Serra, M. E. S. S.,  
421 Tewes, F., Olivier, J.-C. (2015). Optimization of levofloxacin-loaded crosslinked chitosan  
422 microspheres for inhaled aerosol therapy. *European Journal of Pharmaceutics and*  
423 *Biopharmaceutics*, 96, 65–75. <https://doi.org/10.1016/j.ejpb.2015.07.010>
- 424 George, M., & Abraham, T. E. (2006). Polyionic hydrocolloids for the intestinal delivery of  
425 protein drugs: Alginate and chitosan - a review. *Journal of Controlled Release*, 114(1), 1–  
426 14. <https://doi.org/10.1016/j.jconrel.2006.04.017>
- 427 Gómez-Mascaraque, L. G., Sanchez, G., & López-Rubio, A. (2016). Impact of molecular weight  
428 on the formation of electrosprayed chitosan microcapsules as delivery vehicles for bioactive  
429 compounds. *Carbohydrate Polymers*, 150, 121–130.  
430 <https://doi.org/10.1016/j.carbpol.2016.05.012>
- 431 Grenha, A., Seijo, B., Remuñán-López, C. (2005). Microencapsulated chitosan nanoparticles for  
432 lung protein delivery. *European Journal of Pharmaceutical Sciences*, 25, 427–437.  
433 <https://doi.org/10.1016/j.ejps.2005.04.009>
- 434 ICPR. (1994). Human Respiratory Tract Model for Radiological Protection. *Pergamon*, 24(1–3).
- 435 Klinger-Strobel, M., Lautenschläger, C., Fischer, D., Mainz, J. G., Bruns, T., Tuchscher, L., ...  
436 Makarewicz, O. (2015). Aspects of pulmonary drug delivery strategies for infections in  
437 cystic fibrosis-where do we stand? *Expert Opinion on Drug Delivery*, 12(8), 1351–1374.  
438 <https://doi.org/10.1517/17425247.2015.1007949>
- 439 Korsmeyer, R. W., Von Meerwall, E., & Peppas, N. A. (1986). Solute and penetrant diffusion in  
440 swellable polymers. II. Verification of theoretical models. *Journal of Polymer Science Part*  
441 *B: Polymer Physics*, 24(2), 409–434. <https://doi.org/10.1002/polb.1986.090240215>
- 442 Kyzioł, A., Mazgala, A., Michna, J., Regiel-Futyra, A., & Sebastian, V. (2017). Preparation and  
443 characterization of alginate/chitosan formulations for ciprofloxacin-controlled delivery.  
444 *Journal of Biomaterials Applications*, 32(2), 162–174.  
445 <https://doi.org/10.1177/0885328217714352>
- 446 Linder, W.D., Lippold, B. . (1995). Drug release From Hydrocolloid Embeddings with High or  
447 Low Susceptibility to Hydrodynamic Stress. *Pharmaceutical Research*, 12(11).
- 448 Ling, J., Mangal, S., Park, H., Wang, S., Cavallaro, A., & Zhou, Q. T. (2019). Simultaneous

- 449 Particle Size Reduction and Homogeneous Mixing to Produce Combinational Powder  
450 Formulations for Inhalation by the Single-Step Co-Jet Milling. *Journal of Pharmaceutical*  
451 *Sciences*, 108(9), 3146–3151. <https://doi.org/10.1016/j.xphs.2019.05.011>
- 452 Ma, Z., Garrido-Maestu, A., & Jeong, K. C. (2017). Application, mode of action, and in vivo  
453 activity of chitosan and its micro- and nanoparticles as antimicrobial agents: A review.  
454 *Carbohydrate Polymers*, 176(April), 257–265.  
455 <https://doi.org/10.1016/j.carbpol.2017.08.082>
- 456 McShane, P. J., Weers, J. G., Tarara, T. E., Haynes, A., Durbha, P., Miller, D. P., ... Elborn, J. S.  
457 (2018). Ciprofloxacin Dry Powder for Inhalation (ciprofloxacin DPI): Technical design and  
458 features of an efficient drug–device combination. *Pulmonary Pharmacology and*  
459 *Therapeutics*, 50(January), 72–79. <https://doi.org/10.1016/j.pupt.2018.03.005>
- 460 Möbus, K., Siepmann, J., Bodmeier, R. (2012). Zinc-alginate microparticles for controlled  
461 pulmonary delivery of proteins prepared by spray-drying. *European Journal of*  
462 *Pharmaceutical Sciences*, 81, 121–130.
- 463 Moreno, M. A., Gómez-Mascaraque, L. G., Arias, M., Zampini, I. C., Sayago, J. E., Ramos, L.  
464 L. P., ... Isla, M. I. (2018). Electrospayed chitosan microcapsules as delivery vehicles for  
465 vaginal phytoformulations. *Carbohydrate Polymers*, 201(March), 425–437.  
466 <https://doi.org/10.1016/j.carbpol.2018.08.084>
- 467 Osman, R., Kan, P.L., Awad, G., Mortada, N., El-Shamy, A-E., Alpar, O. (2013). Spray dried  
468 inhalable ciprofloxacin powder with improved aerosolisation and antimicrobial activity.  
469 *International Journal of Pharmaceutics*, 449(44–58), 634.
- 470 Pawar, A., Thakkar, S., & Misra, M. (2018). Review article A bird ' s eye view of nanoparticles  
471 prepared by electrospaying : advancements in drug delivery fi eld, 286(July), 179–200.  
472 <https://doi.org/10.1016/j.jconrel.2018.07.036>
- 473 Peppas, N. A., & Sahlin, J. J. (1989). A simple equation for the description of solute release. III.  
474 Coupling of diffusion and relaxation. *International Journal of Pharmaceutics*, 57(2), 169–  
475 172. [https://doi.org/10.1016/0378-5173\(89\)90306-2](https://doi.org/10.1016/0378-5173(89)90306-2)
- 476 Pignatello, R., Leonardi, A., Fuochi, V., Petronio, G. P., Greco, A. S., & Furneri, P. M. (2018).  
477 A method for efficient loading of ciprofloxacin hydrochloride in cationic solid lipid  
478 nanoparticles: Formulation and microbiological evaluation. *Nanomaterials*, 8(5), 1–11.  
479 <https://doi.org/10.3390/nano8050304>

- 480 Qasim, S. B., Zafar, M. S., Najeeb, S., Khurshid, Z., Shah, A. H., Husain, S., & Rehman, I. U.  
481 (2018). Electrospinning of chitosan-based solutions for tissue engineering and regenerative  
482 medicine. *International Journal of Molecular Sciences*, 19(2).  
483 <https://doi.org/10.3390/ijms19020407>
- 484 Tawfik, T. M., & El-Masry, A. M. A. (2021). Preparation of chitosan nanoparticles and its  
485 utilization as novel powerful enhancer for both dyeing properties and antimicrobial activity  
486 of cotton fabrics. *Biointerface Research in Applied Chemistry*, 11(5), 13652–13666.  
487 <https://doi.org/10.33263/BRIAC115.1365213666>
- 488 Thorley, A. J., & Tetley, T. D. (2013). New perspectives in nanomedicine. *Pharmacology &*  
489 *Therapeutics*, 140, 176–185.
- 490 Torres-Giner, S., Ocio, M. J., & Lagaron, J. M. (2008). Development of active antimicrobial fiber  
491 based chitosan polysaccharide nanostructures using electrospinning. *Engineering in Life*  
492 *Sciences*, 8(3), 303–314. <https://doi.org/10.1002/elsc.200700066>
- 493 Tu, H., Lu, Y., Wu, Y., Tian, J., Zhan, Y., Zeng, Z., ... Jiang, L. (2015). Fabrication of rectorite-  
494 contained nanoparticles for drug delivery with a green and one-step synthesis method.  
495 *International Journal of Pharmaceutics*, 493, 426–433.
- 496 Verlee, A., Mincke, S., & Stevens, C. V. (2017). Recent developments in antibacterial and  
497 antifungal chitosan and its derivatives. *Carbohydrate Polymers*, 164, 268–283.  
498 <https://doi.org/10.1016/j.carbpol.2017.02.001>
- 499 Yhee, J., Im, J., & Nho, R. (2016). Advanced Therapeutic Strategies for Chronic Lung Disease  
500 Using Nanoparticle-Based Drug Delivery. *Journal of Clinical Medicine*, 5(9), 82.  
501 <https://doi.org/10.3390/jcm5090082>
- 502